LATERAL VIBRATION REDUCTION IN HIGH PRESSURE CENTRIFUGAL COMPRESSORS

by

Rudolf Jenny

Manager, Research & Development

Turbocompressor Engineering

and

Hans R. Wyssmann

Head of Mechanical Development

Sulzer Brothers Limited

Thermal Turbomachinery

Zurich, Switzerland

Rudolf Jenny graduated Mechanical Engineer at the Federal Institute of Technology in Zürich in 1961. He obtained his degree of "Docteur Ingénieur" from the Faculté des Sciences de l'Université de Paris in 1965. For several years he was involved in research work in the Wind Tunnel Department of the Swiss Aircraft Factory near Luzern. In 1975 he joined Sulzer Brothers' Turbocompressor Department in Zürich, Switzerland. Since January 1976 Dr. Jenny has held the post of manager in the Development Section of this department. He is responsible for the aero-thermodynamic and mechanical development of industrial turbocompressors, both axial and centrifugal.

Hans R. Wyssmann graduated in Mechanical Engineering from the Federal Institute of Technology in Zürich in 1970 and then spent a year at the Georgia Institute of Technology where he received a M.S. degree in Engineering Mechanics. After returning to Switzerland, he was active in research and teaching in applied mechanics at the Federal Institute of Technology and received his Ph.D. there in 1979. Since then Dr. Wyssmann has been working for Sulzer Brothers Ltd. where he is responsible for the mechanical development of turbocompressors. His work includes the investigation of the mechanisms of forced and self-excited vibrations of rotors and optimization of rotor design with respect to lateral vibrations.

ABSTRACT

Recent designs of high and medium pressure centrifugal compressors show a well-behaved response to forced vibration and an adequate margin to self-excited vibration. This can only be achieved by an extensive rotor dynamic analysis and wide practical experience. A number of sophisticated computer codes to calculate the response and the stability of complex rotors are widely used. One problem with the application of these programs is the realistic estimation of data for aerodynamic excitation. It is the purpose of this paper to discuss the different types of excitation that occur in a multistage centrifugal compressor with shrouded impellers and to evaluate their importance with respect to lateral vibrations. The main source for self-excitation is found to be the labyrinth seals. A simple one-dimensional aerodynamic theory to calculate the destabilizing lateral forces of the labyrinths is presented. It is shown that the tangential velocity of the leakage gas strongly influences the excitation. Simple devices which may be installed in nearly any compressor reduce the excitation by reducing the fluid rotation in the labyrinth annulus.

Stability tests for a number of different centrifugal compressors have been carried out on a test bed. The stability limits have been determined by increasing the pressure level at constant speed until subsynchronous vibration occurs. The measured stability limits agree well with those theoretically predicted using calculated labyrinth data.

INTRODUCTION

By lateral vibrations we mean the translatory oscillations of the axis of the rotor in the planes orthogonal to the axis of rotation. The torsional vibrations of the rotor and the vibration of the blades and their interaction with the rotor are not considered here. The rotor interacts with its bearings and their supports and their influence has in general been taken into account when analyzing the dynamics of the rotor. Sophisticated computer codes are available and widely used to simulate this vibratory system.

The rotor is generally the best known part of this system. It is usually modeled as a Timoshenko beam with concentrated masses which possess translatory and gyroscopic inertia. This technique provides a realistic representation of the actual rotor, if a sufficient number of discrete mass stations are employed.

The bearings, almost exclusively fluid film bearings, form a massless spring-damper system. In high pressure applications the tilting pad bearing is used almost without exception due to its excellent properties with regard to self-excitation. The stiffness and damping properties of tilting pad bearings for high speed rotors with moderate weights (i.e., at Sommerfeld number higher than 1.0) are often isotropic. These bearings may therefore be simply described by two coefficients: one for stiffness and one for damping. In the following, tilting pad bearings will be assumed to be isotropic. There are many computer programs for the calculation of bearing coefficients. All of them are based on the linearization of Reynold's equation about the equilibrium position of the rotor. Our experience shows good agreement between the calculated and the

measured bearing characteristics for tilting pad bearings. This becomes apparent in Figure 1, where the measured and calculated amplitudes of forced vibrations in the vicinity of the second critical speed due to a known antisymmetric unbalance are shown. The vibrations of a centrifugal rotor with tilting pad bearings have been measured on the high speed balancing machine shown in Figure 2. The bearings pedestals were modeled as single mass systems with modal parameters obtained by experimental modal analysis. The good agreement between measured and calculated amplitudes essentially confirms the calculated bearing coefficients. This enables a rotor design to be selected that has a favorable dynamic behaviour complying with the user's specifications.

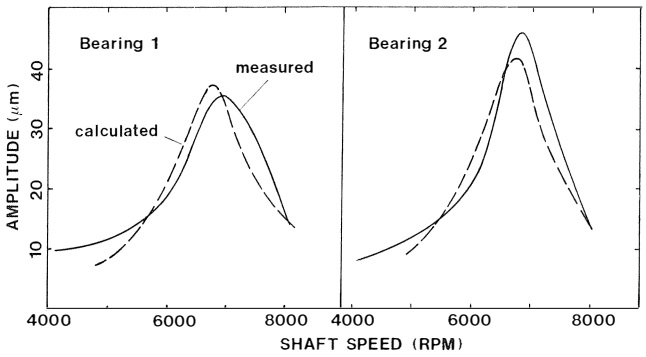

Figure 1. Calculated and Measured Forced Vibration Response.

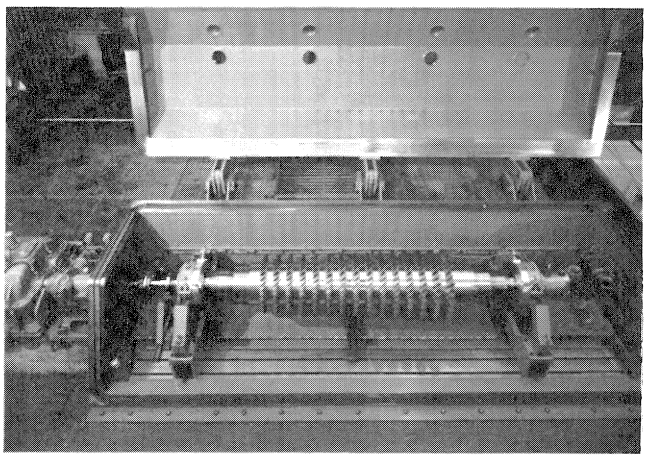

Figure 2. High Speed Balancing Machine.

Discrepancies have been found for fixed lobe bearings of the lemon type possessing cross-coupling stiffness and damping. In particular the theoretically predicted damping does not coincide with that obtained from measurements. The problem seems to be connected with the high Sommerfeld number, where linearization for fixed lobe bearings becomes problematic.

The bearing support includes the bearing pedestal, compressor casing and foundation and is the part of the vibratory system which is the most difficult to simulate. For high pressure compressors with their stiff casings and pedestals and light-weight rotors, its influence on the vibrations of the rotor may be neglected by assuming rigid bearing supports. For large axial compressors, investigations of the flexibility of the bearing supports have been made. Figure 3 shows the mobility functions in the horizontal and vertical directions measured in one of the bearing planes. Simulation of such complex systems is achieved with lumped masses that are determined with the aid of modal analysis techniques. However, this is a laborious procedure. A more appropriate way would be to describe the mobilities by complex rational functions and use them directly in suitably adjusted computer programs for rotor dynamics. Unfortunately, such programs which are industrially applicable are not available. In some cases, it is sufficient to model the bearing supports by single mass systems valid only in a narrow frequency band.

The vibratory system, thus defined, may be investigated with the aid of computer programs which calculate the:

- undamped natural frequencies, often identified with the critical speeds,
- amplitude of the forced vibrations and
- eigenvalues of the system taking into account the damping and self-excitation mechanisms.

CRITICAL SPEEDS

Critical speeds, according to API Standard 617 [1,2], are defined as the speeds where resonance of the rotor-bearing system occurs. This is the case whenever the rotor speed is close to a natural frequency of the rotor-bearing system. The critical speeds are thus identified with the natural frequencies of the system. Actually three different quantities have to be distinguished:

- the undamped natural frequency ω_0, usually calculated with the aid of the critical speed map,
- the damped natural frequency ω_d, given by the imaginary part of the system eigenvalues,
- the frequency of maximum vibration amplitude ω_{max}.

The relations between them as functions of the logarithmic decrement of the system damping δ are given in Figure 4, together with the maximum amplitude magnification β. In practice the important quantity is the frequency of maximum vibration amplitude ω_{max}. The first critical speed usually has a δ value of less than 0.5. In this case, ω_{max} differs by less than 1% from the undamped natural frequency ω_0, which usually is calculated as an estimate for the critical speed. The second critical speed in high pressure compressors, however, may have a damping δ value of more than 2. The difference between ω_0 and ω_{max} is then 10% or more. A realistic prediction of critical speeds should, therefore, consist of the calculation of the forced vibration response.

With high system damping, the amplitude magnification is small and may hardly be observed, especially if the unbalance excites other, less damped modes. Moreover, the

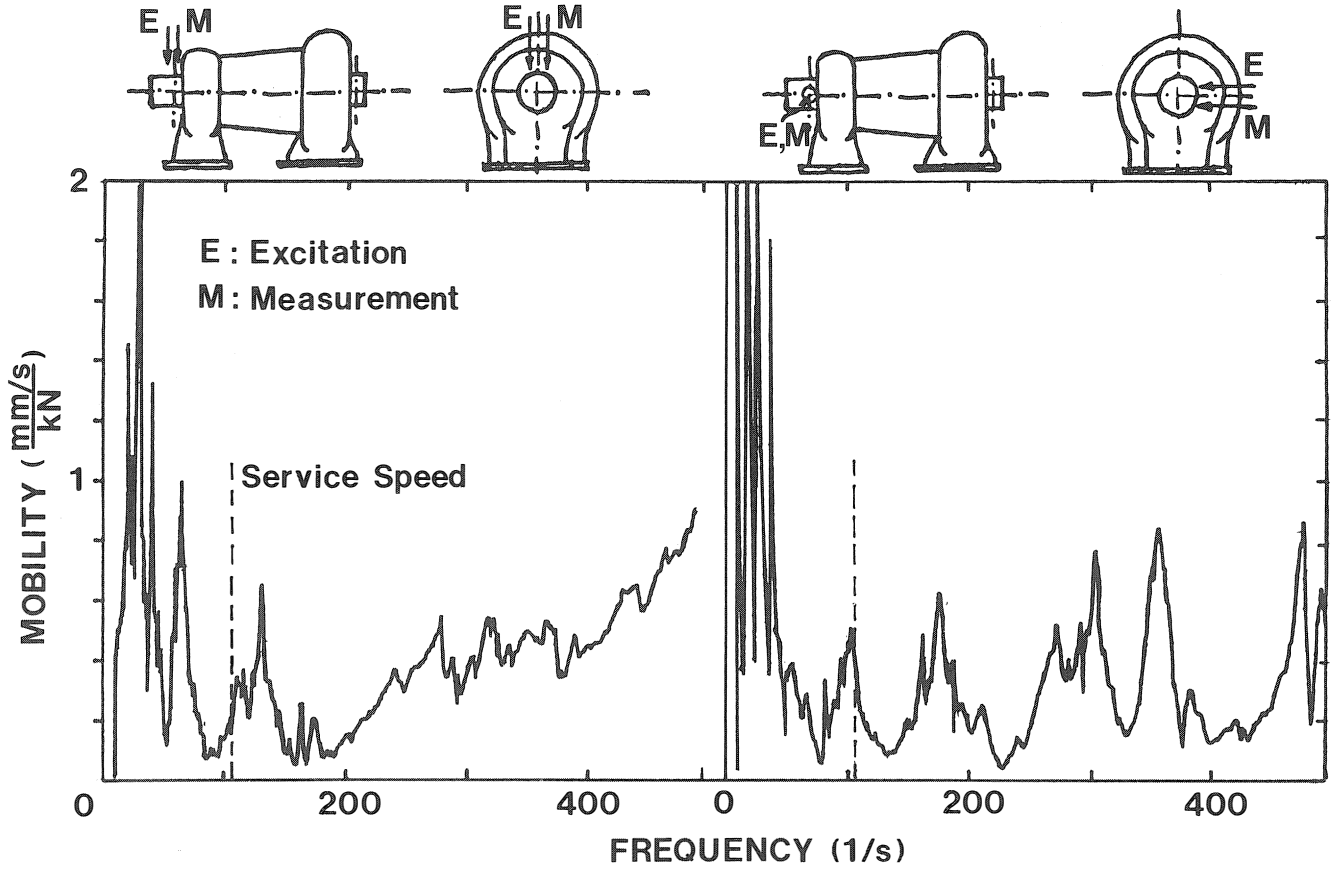

Figure 3. Mobilities of Bearing Support.

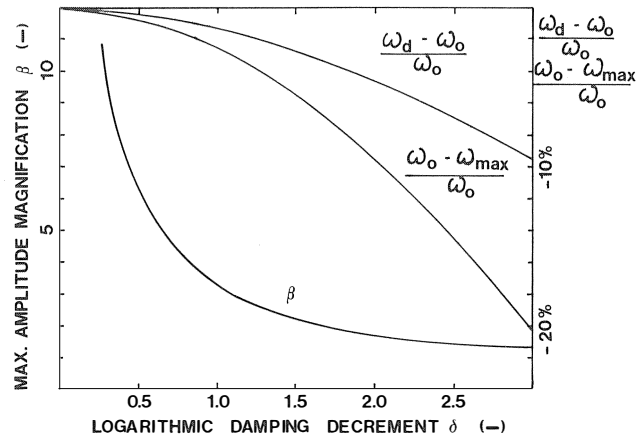

Figure 4. Influence of Damping on Critical Frequencies and Amplitude Magnification.

location of the maximum amplitude may be dependent on the unbalance and the measuring planes, since coupling of the modes due to damping becomes important. This is especially true for the highly damped second and usually less damped third mode.

STABILITY ANALYSIS

The equilibrium position of the rotor may become unstable by self-exciting mechanisms which convert rotary energy into translatory energy. The resulting vibration has a frequency which is close to or identical with a natural frequency of the system. The stability analysis of a rotor-bearing system leads to an eigenvalue problem. Powerful computer programs are available which calculate the eigenvalues from which the damped natural frequencies and the stability margins may be determined.

The numerically calculated eigenvalues form a finite series of complex conjugate numbers:

$$\lambda_k = \mathrm{Re}(\lambda_k) + i\,\mathrm{Im}(\lambda_k) \quad . \tag{1}$$

The damped natural frequencies are given by the absolute values of the imaginary parts of the eigenvalues:

$$\omega_k = |\mathrm{Im}(\lambda_k)| \quad , \tag{2}$$

and the damping, expressed by the logarithmic decrement, reads:

$$\delta_k = -2\pi \frac{\mathrm{Re}(\lambda_k)}{\omega_k} \tag{3}$$

The rotor is stable if all the real parts of the eigenvalues are negative; i.e., if all the δ_k's are positive. If one of the logarithmic decrements δ_k is negative, the rotor becomes unstable. As a rule, it is the first eigenvalue which may show instability, being the most sensitive to excitation.

Most of the self-exciting mechanisms, and among them the important ones, may be conceived as forces acting on the rotor which are orthogonal to and linear in the rotor displace-

ment. They are often called lateral forces. Figure 5 shows a section through a rotor which is displaced by the radial distance r from the equilibrium position 0. The force acting on the rotor due to the displacement is given by the radial component R and the tangential component Q. The radial component R is caused mainly by the rotor and bearing stiffness and has no contribution to self-excitation. The tangential component Q, however, may cause a destabilization of the rotor if the damping in the system is not sufficient. The ensuing motion describes an outwardly oriented spiral in the direction of Q. Depending on the physical nature of the mechanism causing Q, its orientation may be equal or opposite to that of the shaft speed. If there are several causes for Q, it is the sum of the influences of all the Q's which decides upon stability and the direction of the self-excited motion. Thereby cancellation of different mechanisms is possible. In Cartesian coordinates the lateral force Q_i at rotor station i may be represented by their components Q_{x_i} and Q_{y_i} which are given by

$$Q_{x_i} = -k_i y_i \qquad Q_{y_i} = k_i x_i \tag{4}$$

where x_i, y_i: rotor displacements at rotor station i,
k_i: cross-coupling stiffness at rotor station i.

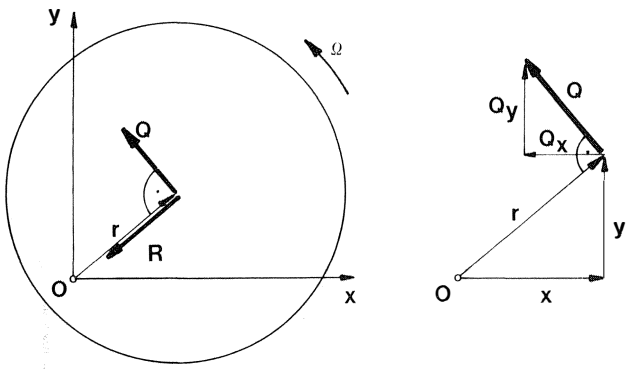

Figure 5. Forces Acting on the Rotor.

Figure 6 shows the dependence of the system damping δ on the sum k of the cross-coupling stiffnesses k_i for some medium and high pressure centrifugal compressors. The calculations were made by a commercial computer program with a distribution of the k_i's along the rotor given by the labyrinth excitation model presented later. First of all, it can be seen that δ is almost linearly dependent on k for the rotors with tilting pad bearings, when the stiffness and damping are isotropic. This is not true when anisotropic bearings are used as example 5 in Figure 6 shows. The linear δ-k dependence for isotropic or nearly isotropic rotor-bearing systems simplifies the stability analysis in that only two points of the δ-k curve have to be calculated.

Rotors 1 through 3 in Figure 6 have roughly equal overall dimensions due to their similar mass flow. Therefore, although their dampings at zero excitation are different, they have similar sensitivities to excitation, i.e., similar derivatives dδ/dk. Rotor 4, however, is of much larger size and shows, therefore, a largely different excitation dependence compared to the others.

The intersection of the δ curve with the k-axis give the critical excitation k_{crit}, i.e., the excitation where instability

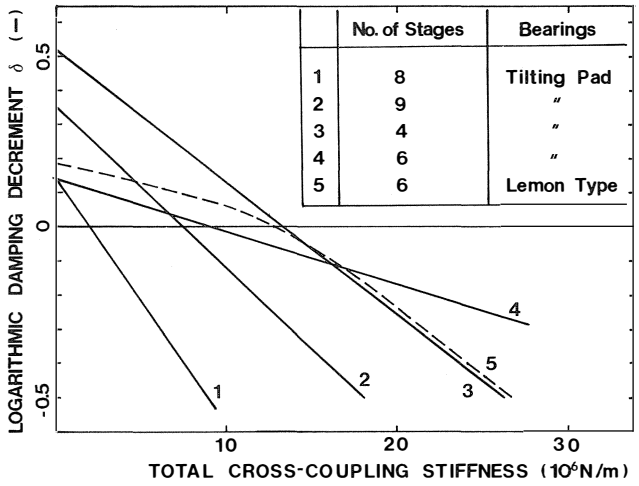

Figure 6. Dependence of System Damping on Excitation.

begins. The critical excitation must of course be higher than the excitation in service in order to avoid instability. Figure 7 shows the influence of design parameters, i.e., the number of stages, impeller diameter and circumferential speed on the critical excitation. With information like this, it is possible to select a rotor design with favorable properties with regard to stabilty if the service excitation is known.

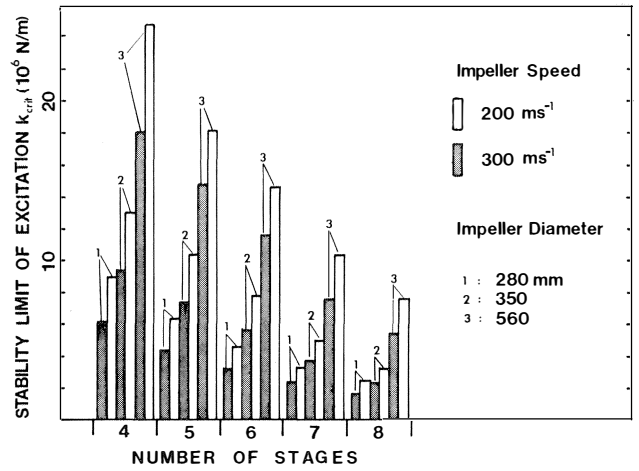

Figure 7. Influence of Design Parameters on Stability Limit.

For parameter studies involving several parameters, the computer costs may become substantial. Therefore, an explicit approximate formula for δ has been derived in the Appendix. It is valid for isotropic rotor-bearing systems with an error of a few per cent if δ at zero excitation is less than 0.6. Figure 8 shows a parameter study of δ for a high pressure natural gas compressor designed for an end pressure of 320×10^5 N/m^2 (320 bar). For a given service excitation of 13×10^6 N/m, the logarithmic damping decrement δ as a function of bearing stiffness c and bearing damping d has been calculated with formula (A-4). It is seen that for a given bearing damping, an optimal value for the bearing stiffness exists. Further analysis shows even the existence of a global optimum, i.e., of a maximum value of δ for a certain pair of bearing stiffness and

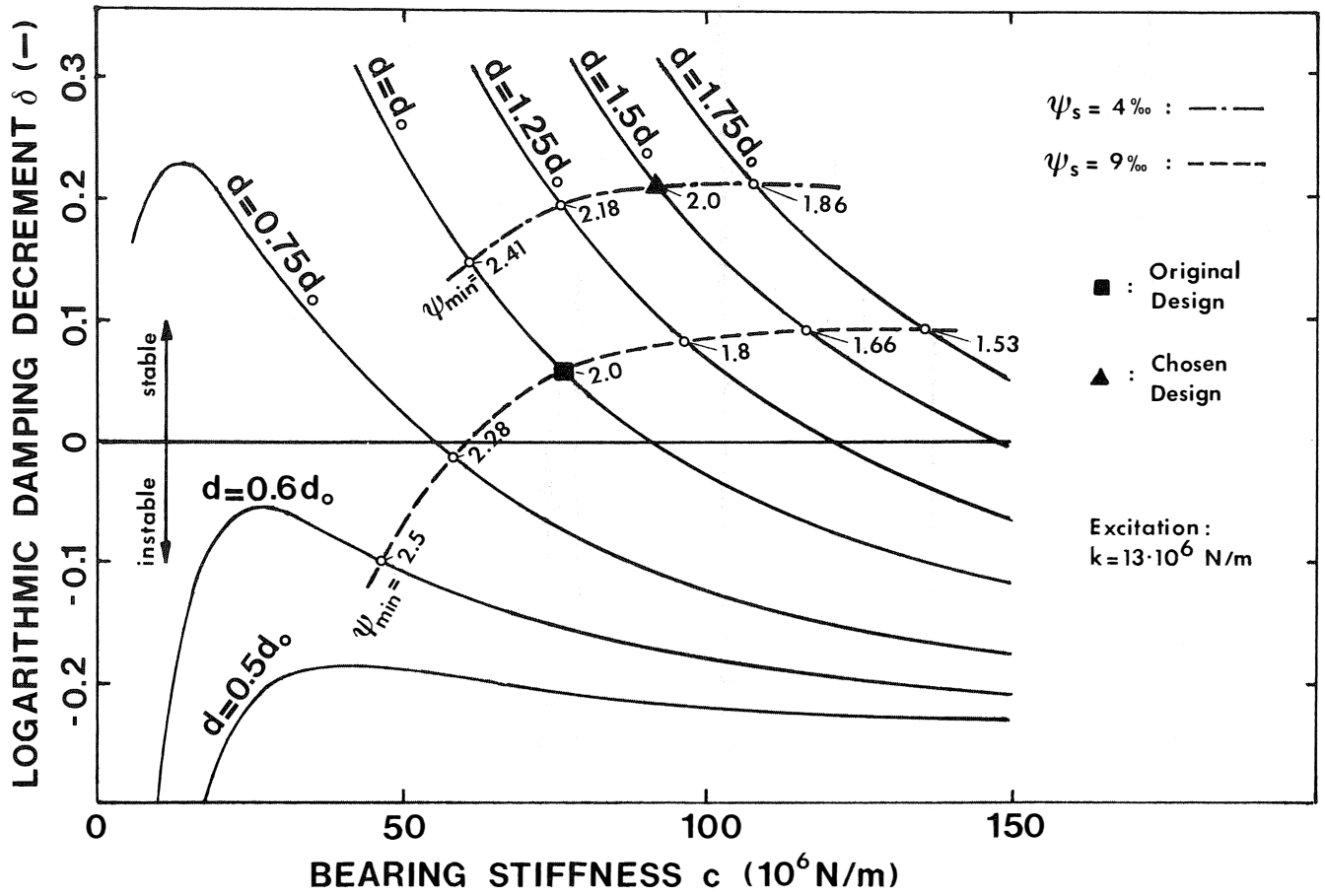

Figure 8. Influence of Bearing Parameters on System Damping.

damping. Current bearing designs cannot yield optimal values due to physical and economical reasons, but even minor design changes may substantially improve the stability margin, as Figure 8 makes clear. The finally chosen bearing design with a minimal radial bearing clearance ψ_{min} of 2% is an optimum for the pad clearance ψ_s of 4%.

FORCED VIBRATIONS

Forced vibrations are defined as the steady-state oscillations of a system caused by a periodic excitation. The most common cause is unbalance of the rotor. By a refined balancing technique its influence may be reduced to a minimum. The impellers are balanced separately prior to mounting on the rotor. In order to compensate the systematic error caused by the impeller balancing equipment the impellers are mutually rotated by 180 degrees while being mounted on the rotor. Finally the rotor with the mounted impellers is balanced on the high speed balancing machine seen in Figure 2 by a multiple plane method. This procedure ensures a high quality standard of balancing with hardly noticeable residual unbalance.

Besides unbalance, aerodynamic excitations like surge and rotating stall may be causes for forced vibrations. According to the compressor design, the flow may become locally unstable exhibiting rotating stall or instabilities of the whole compressor circuit when surge occurs. Surge is in no case an accepted mode of operation and the compressor must be protected by some kind of anti-surge device.

Rotating stall is a well-known phenomenon in axial compressors. Experience has shown that a similar mechanism may occur in centrifugal compressors as well, with vaned and vaneless diffusers. It is generally limited to a particular stage and usually has its origin in the diffuser. Surge occurs when the flow angle to the diffuser falls below a critical value. As can be seen from single stage tests this usually coincides with the drop of pressure recovery in the diffuser. The characteristics shown in Figure 9 were obtained by testing a standard stage with a

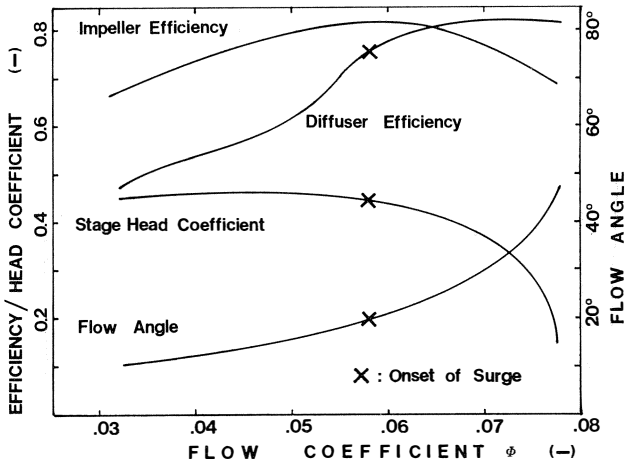

Figure 9. Onset of Surge.

vaneless diffuser. Rotating stall sets in at a flow angle of about 20 degrees. The rotating flow field associated with stall often yields a revolving force which excites the rotor. Usually the rotating stall frequency is much lower than the first natural frequency of the rotor thereby causing only small vibration amplitudes unless the gas density is high. It follows that for high pressure centrifugal compressors it is important to match impellers to the diffusers, as well as the different stages, in such a way that diffuser rotating stall does not occur before the compressor reaches its surge limit.

SELF-EXCITED ROTOR VIBRATIONS

This type of vibration is often called rotor whirl or subsynchronous vibration. The latter designation is misleading since forced vibrations may also be subsynchronous with respect to the rotor speed. It is actually a destabilization of the equilibrium position of the rotor. There exists a large number of mechanisms which theoretically may cause self-excitation, or at least contribute to it. This is one explanation why the opinions about this subject are so contradictory. Before arriving at the labyrinth seal excitation, some of the less important mechanisms are looked at in the following.

Internal damping of the shaft and shrink fits of impellers may give rise to excitation if the rotor is operating above the first critical speed which is practically always the case. Estimations by different authors [3,4] show that internal damping gives only a small contribution to self-excitation compared with the labyrinth seal excitation presented later. Shrink fits of impellers may have a similar effect. However, it may be practically eliminated by an appropriate rotor design which reduces the friction between impeller and rotor.

Aerodynamic whirl excitation is related to lateral aerodynamic forces due to varying tip clearances when the rotor is displaced from the center position. The phenomenon was first encountered in steam turbines and has been described under the name steam whirl by Thomas [5] and Alford [6]. It has been conjectured that a similar mechanism also exists in centrifugal impellers of shrouded or unshrouded type. In order to find out the magnitude of this effect, tests with a typical high-pressure impeller were carried out. The torque for concentrically placed impellers with different radial clearances s was measured. As only very small changes in torque were found, a highly sensitive and accurate torque measuring device had to be used. Figure 10 shows the measured work input characteristic μ for a clearance variation $\Delta s/2R$ of 0.02, R being the impeller radius. The change of work input $\Delta\mu$, being by definition proportional to the change of torque, gives a corresponding change of a tangential force per radian Δf:

$$\Delta f = \frac{2\rho u^2 R^2 \phi}{\pi} \Delta\mu, \tag{5}$$

where ρ: gas density,
u: circumferential impeller speed,
ϕ: flow coefficient.

Given a small eccentricity e of the impeller, the clearance variation Δs may be written:

$$\Delta s = e\cos\varphi, \tag{6}$$

where φ is measured from the place of maximum clearance. Dividing equation (5) by Δs and using equation (6), it follows, after integration for the force component Q orthogonal to the eccentricity, that

$$Q = 2\rho u^2 R^2 \phi \frac{\Delta\mu}{\Delta s} e. \tag{7}$$

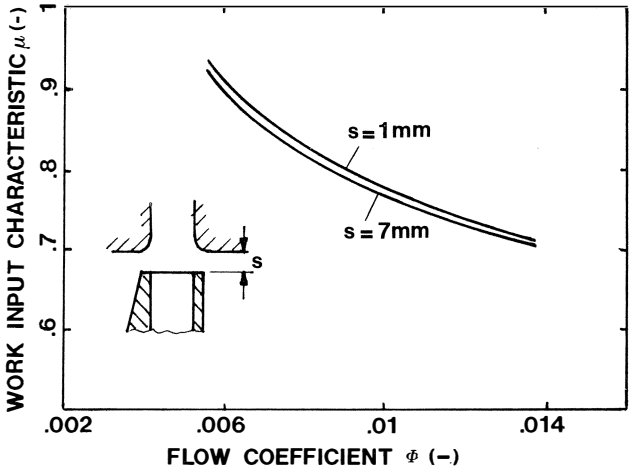

Figure 10. Work Input Characteristics.

With the following relations valid for ideal gases

$$\frac{P}{\rho} = RT, \quad a = \sqrt{\gamma RT}$$

where a is the speed of sound. Writing $M_u = u/a$ for the impeller Mach number, equation (7) leads to a dimensionless cross-coupling stiffness:

$$\frac{Q}{epR} = 2\gamma M_u^2 \phi R \frac{\Delta\mu}{\Delta s} \tag{8}$$

Using the test results and $\gamma = 1.4$ for air, equation (8) gives

$$\frac{Q}{epR} = 0.005 \tag{9}$$

This is about two orders of magnitude smaller than the cross-coupling stiffness due to labyrinth seal excitation, as will be seen later.

Self-excited rotor vibrations due to fluid film bearings, known as oil whirl and oil whip, have been known for a long time. Multi-lobe bearings and especially the tilting-pad bearing have virtually eliminated this problem. Nevertheless, due to the fact that the bearing is practically the only source of damping in the system, it has to be carefully selected in order to have a sufficient rotor stability margin.

Floating ring seals can act in a similar manner as journal bearings and thus potentially contribute to self excitation. The analogy to a circular short bearing is quite obvious and the corresponding theories allow their stiffness and damping properties in the locked-up position to be determined. Floating ring seals are held radially only by friction forces, which allow them to follow the shaft motion as long as the friction is overcome. A stability analysis with the seals in the locked-up positions is therefore generally too pessimistic. Nevertheless it allows one to estimate the effect of floating ring seals on the rotor dynamics. Constructively, the destabilizing effect may be reduced by balancing the ring in such a way that the axial force on the seal, and hence the friction forces, are as small as possible. Another possibility is to optimize the clearance geometry in order to obtain favorable dynamic stiffness properties.

Self-excitation due to Labyrinth Seals

Several authors have experimentally verified that labyrinth seals influence the stability of rotors. However, the importance of this effect in high pressure centrifugal compressors has not yet been fully recognized.

Measurements have been made by Roseberg, et. al. [7] and recently extensive experimental investigations have been carried out by Benckert [8]. He measured the pressure distribution around the labyrinth of an eccentrically positioned rotor and by integration, he obtained the lateral force appertaining to the corresponding rotor eccentricity. His findings showed that the resulting cross-coupling stiffness heavily depends on the labyrinth geometry as well as on the operating conditions. An extrapolation of his results to other geometries, pressure levels, molecular weights, etc., leads to unrealistically high values of excitation, which could not be found in real compressors. A physically correct theoretical model is therefore urgently needed. Earlier attempts to calculate the excitation of labyrinths by Alford [6], Kostyuk [9], Spurk [10], Rosenberg [7] and Urlichs [11] were either not successful in predicting quantitatively correct cross-coupling stiffnesses or did not predict a destabilizing effect at all.

Theoretical Model

The starting point of the theoretical investigation is the flow in the *concentric* labyrinth. It is rather complex, consisting not only of the separated meridional flow behind the labyrinth strips but also of tangential flow components due to the swirl of the entering leakage flow and the rotation of the shaft. Finite element flow calculations using the k-ε turbulence model [12] allow the calculation of the complete rotationally symmetric flow field. It can be seen that the tangential flow consists of an extended core-flow with only thin boundary layers at the rotating and stationary surfaces and a thin shear layer at the free boundary to the leakage flow passing through the labyrinth as a nearly two-dimensional jet. This is illustrated in Figure 11. Four different flow regions are assumed to exist:

A. Coreflow, having nearly constant tangential velocities.

B. Boundary-layers at the stationary and rotating surfaces, causing friction.

C. Jet flow of the leaking fluid passing through the labyrinth chamber.

D. Mixing region between jet and core-flow.

The average mass flow, pressure and density in each labyrinth channel are computed by the well-known labyrinth equations [13]. The average tangential flow velocity $\overline{w}$ in the core A of the concentric labyrinth is obtained by formulating the equilibrium between the different friction forces and the momentum exchange in the mixing region of the jet. Some assumptions about these friction forces and the momentum exchange have been made, backed by the finite element calculations, in order to calculate $\overline{w}$ for an individual labyrinth as a function of its geometry and operating conditions.

If the labyrinth seal operates *eccentrically*, the tangential velocity w is no longer constant around the labyrinth. For a small rotor displacement e in the direction $\varphi = \pi$ as depicted in Figure 12, the core velocity $\overline{w}$ is smaller at $\varphi = 0$ than at $\varphi = \pi$. The change in velocity is partly a consequence of the change in cross-section and partly it is related to the circumferentially varying momentum exchange with the traversing jet flow due to the varying clearance. This change of tangential velocity around the eccentric labyrinth causes correspondingly changing friction losses which in turn modify the circumferential pressure distribution as illustrated in Figure 12. It is easily

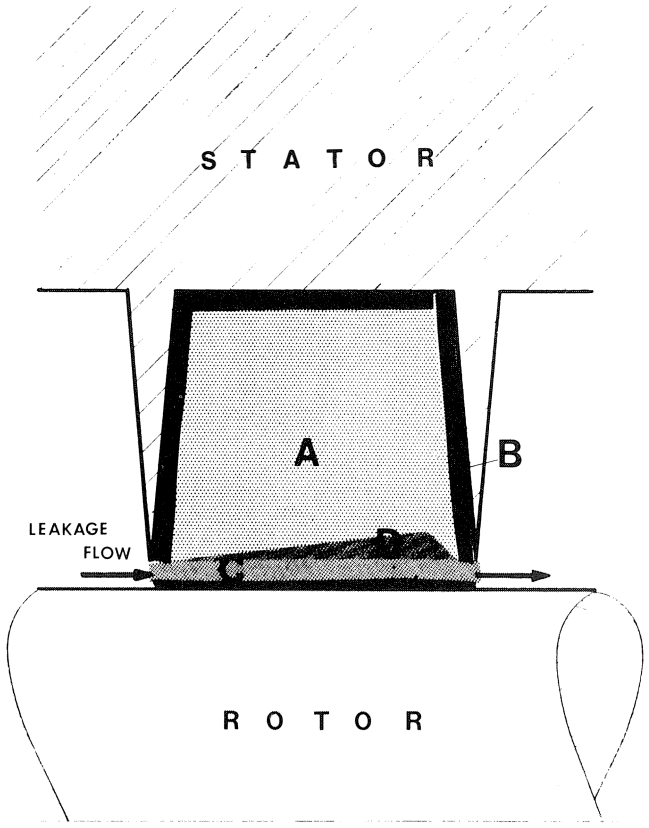

Figure 11. Flow Regions in the Labyrinth.

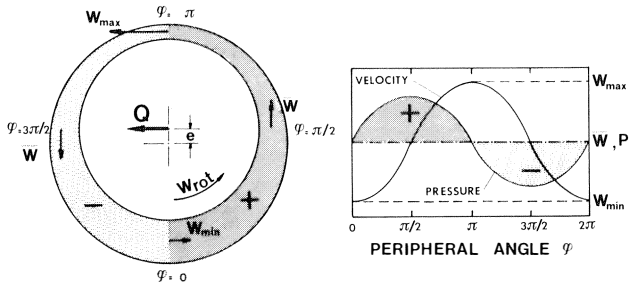

Figure 12. Velocity and Pressure Distribution in the Labyrinth.

seen that the anti-symmetric pressure distribution causes a lateral force Q which has the tendency to self-excite the rotor in a forward direction with respect to the shaft rotation.

Figure 13 shows a comparison between measured and calculated dimensionless cross-coupling stiffness $\frac{Q/e}{p_0 R}$ for a few labyrinths. The experimental values for the labyrinths (a) and (b) stem from Benckert's investigation [8]. The labyrinth (c) is a shroud labyrinth used on a low pressure centrifugal impeller. The cross-coupling stiffness was measured in a single stage test stand with the impeller operating at different flow coefficients and Mach numbers. The good agreement between calculated and measured data confirms the theoretical model, at least in the low pressure range, where the measurements were made. A confirmation for high pressures is given by the stability tests on real compressors described later.

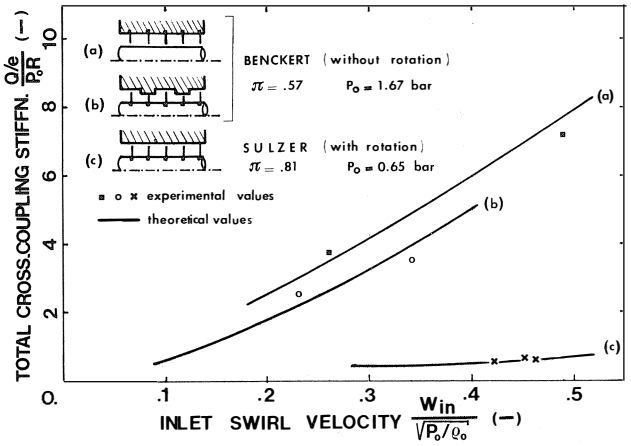

Figure 13. Measured and Calculated Cross-Coupling Stiffness.

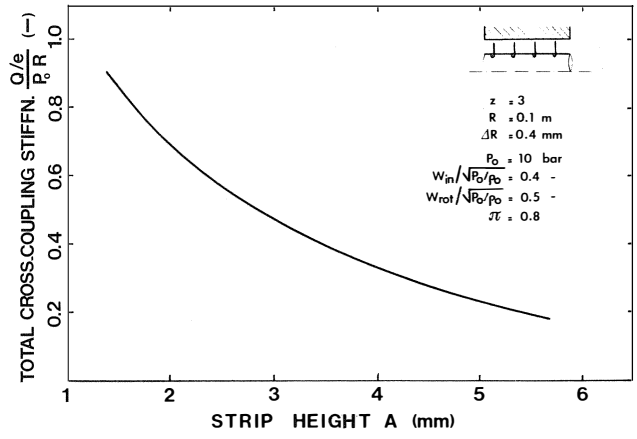

Figure 15. Influence of Strip Height on Cross-Coupling Stiffness.

Parameter Study of Labyrinth Excitation

A computer program based on the flow model just portrayed was used to investigate the influence of different labyrinth goemetries, operating conditions and gas properties on the cross-coupling stiffness. From the large number of parameters affecting labyrinth excitation, a selection which is of practical interest will be presented.

The effect of variation in the *main geometrical dimensions* of a shroud labyrinth, such as radius R, strip height A and labyrinth clearance ΔR is investigated for the following dimensionless operation parameters:

speed of rotation	$W_{rot}/\sqrt{p_0/\rho_0}=0.5,$
swirl velocity	$W_{in}/\sqrt{p_0/\rho_0}=0.4,$
pressure ratio	$\pi=0.8.$

The results shown in Figures 14, 15 and 16 make clear that a reduction in labyrinth diameter and an increase in strip height will result in a significant reduction of excitation, whereas the variation in labyrinth clearance hardly shows any influence.

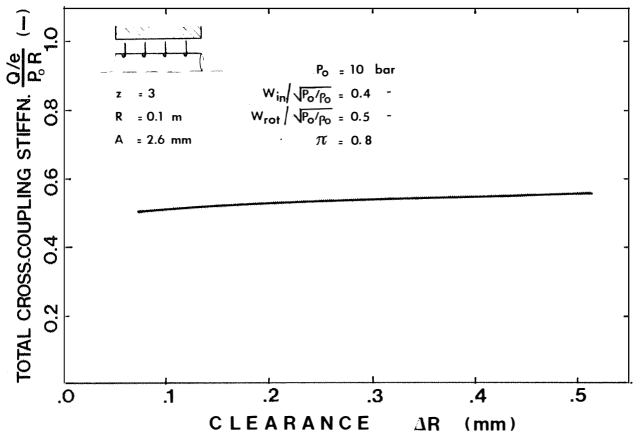

Figure 16. Influence of Labyrinth Clearance on Cross-Coupling Stiffness.

The *operating conditions* also have a major influence on the magnitude of excitation as illustrated in Figures 17 and 18. An increase of rotational speed and swirl velocity aggravate the

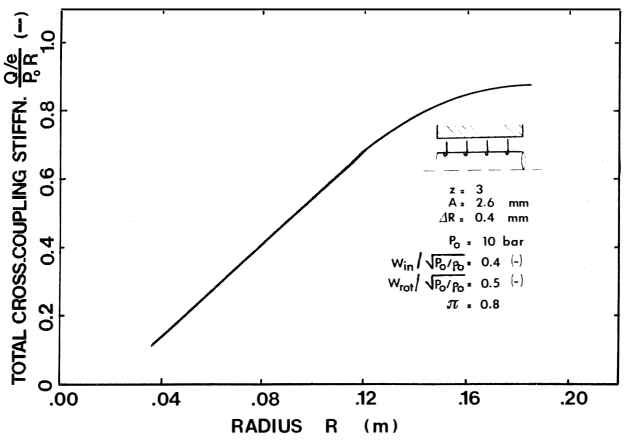

Figure 14. Influence of Labyrinth Radius on Cross-Coupling Stiffness.

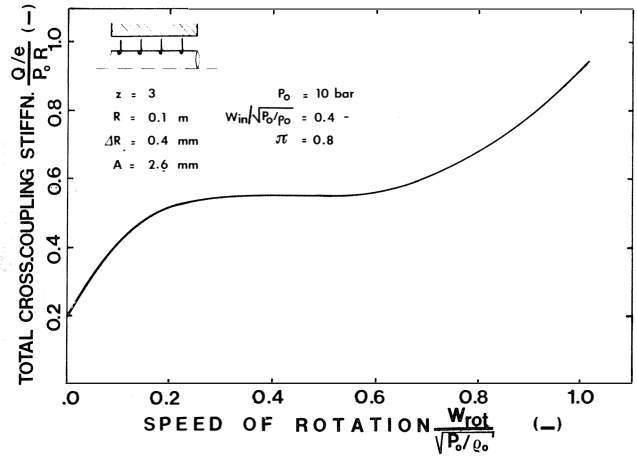

Figure 17. Influence of Rotor Speed on Cross-Coupling Stiffness.

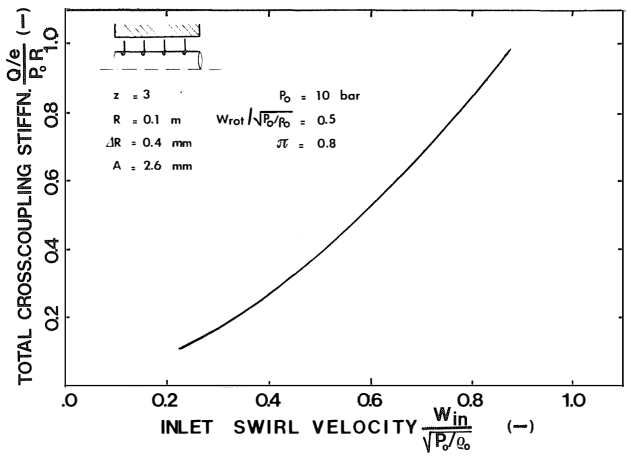

Figure 18. Influence of Swirl Velocity on Cross-Coupling Stiffness.

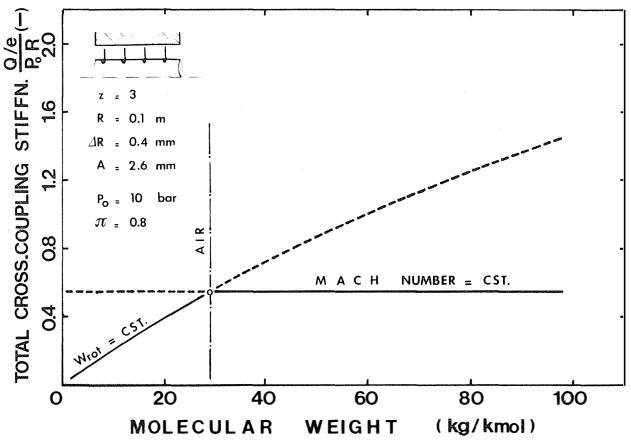

Figure 20. Influence of Mach Number on Cross-Coupling Stiffness.

excitation; the pressure ratio, however, is of minor importance at least for this type of labyrinth as seen in Figure 19.

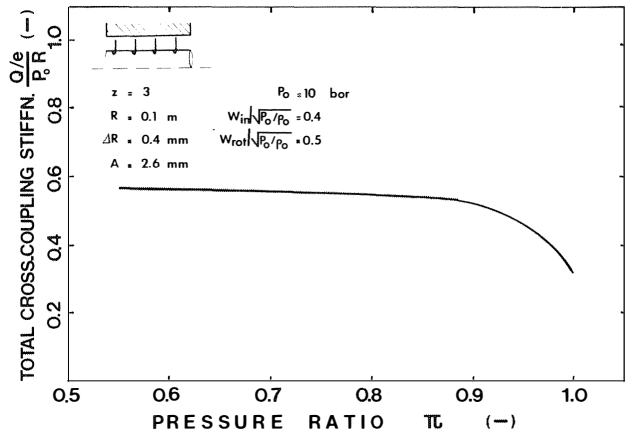

Figure 19. Influence of Pressure Ratio on Cross-Coupling Stiffness.

The model allows equally well to answer the important question in practice of how the *gas properties* affect the cross-coupling stiffness. Let us assume that the maximum speed of a particular impeller, given by the strength of material, coincides with the speed given by the highest acceptable Mach number in air. Two different cases have then to be considered:

1. If this impeller is used with gases heavier than air, the speed must be reduced in order to respect the aerodynamic limitations of the impeller Mach number; that is, the Mach number must be kept constant. Therefore the speed parameters $W_{rot}/\sqrt{p_0/\rho_0}$ and $W_{in}/\sqrt{p_0/\rho_0}$, being directly related to the Mach number, remain the same as for air. The cross-coupling stiffness Q/e is then directly proportional to the pressure before the labyrinth as can be seen in Figure 20.
2. If gases lighter than air are used, the impeller Mach number is reduced while the impeller speed is kept constant. This reduces the speed parameter by the same ratio. The cross-coupling stiffness Q/e then follows the curve W_{rot} = constant in Figure 20, being at the same time proportional to the pressure and roughly proportional to the molecular weight. This has been verified by correlating experimental results obtained on an ethylene compressor.

Verification of the Excitation Model by Stability Tests

The labyrinth excitation model just presented, although confirmed by laboratory tests at low pressures, as shown in Figure 21, stands or falls with its ability to predict stability margins in real compressors. Since the logarithmic damping decrement δ itself is not measurable by today's means, one has to confine oneself with the measurement of the critical pressure, i.e., the pressure at which instability begins. This is, however, not always possible since compressors are designed to run stable in the operational pressure range. Therefore testing at pressure levels substantially higher than design pressure is seldom practicable. Sometimes it is possible to lower the critical pressure level by selecting bearings with lower damping or by changing other design properties for testing purposes.

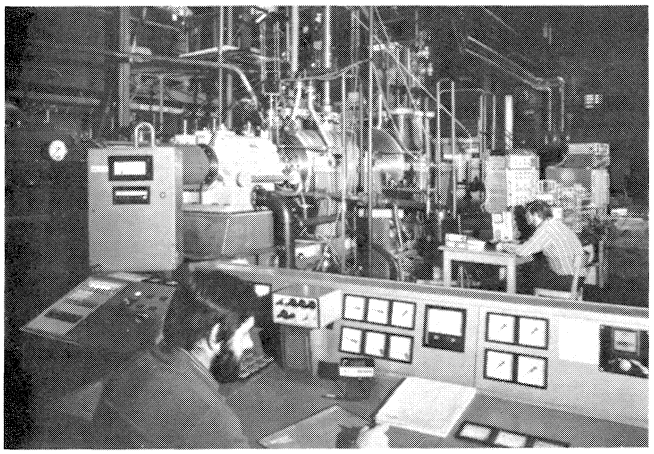

Figure 21. High Pressure Test.

For a specified compressor with a fixed Mach number the labyrinth excitation model gives a linear dependence of the total cross-coupling stiffness k on the end pressure p. The system damping δ as a function of k is given by a sensitivity analysis as shown in Figure 6. Combining the δ-k and the k-p curves gives the dependence of δ on the pressure p at constant Mach number. Figure 22 shows this for the compressors 1, 2 and 4 in Figure 6. The intersection of the δ-curve with the p-axis gives the critical pressure p_{crit}, where the onset of instability has to be expected. The linear stability theory predicts a well defined, sharp stability limit, i.e., a critical pressure p_{crit} above which the vibration amplitude grows unboundedly. Nonlinear and stochastic effects obscure this phenomenon by producing a smooth, although sudden, transition from stability to instability. Thus one has to settle for an appropriate definition of the critical pressure in practice. It seems reasonable to take the vibration-controlled shut-down pressure. The measured p_{crit} values given in Figure 22 are based on this definition. The comparison with the theoretical values shows good coincidence with a deviation of less than 10%. Together with the laboratory measurements this confirms the validity of the theoretical model.

Reduction of Labyrinth Excitation

The theoretical model of labyrinth excitation may be used to optimize the geometrical labyrinth design in order to reduce the excitation. This may possibly allow an additional stage to be placed in a compressor casing without reducing the stability margin.

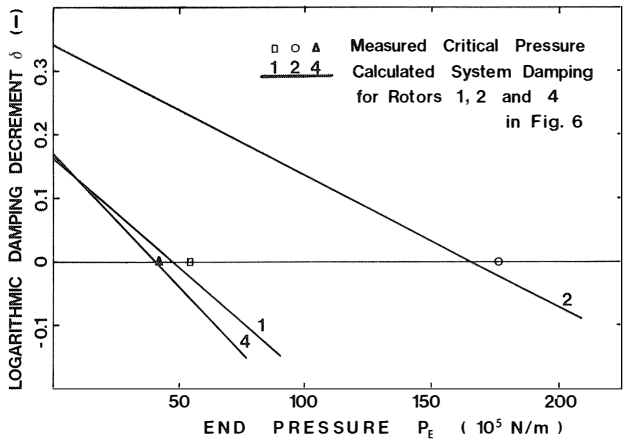

Figure 22. Dependence of System Damping on End Pressure.

If for any reason the stability margin of a compressor in operation is found to be too small, an investigation of the labyrinth excitation may be worthwhile. Very often the dimensionless swirl velocity $W_{in}/\sqrt{p_0/\rho_0}$ of the entering leakage flow is of the magnitude of 0.4, causing the relatively large excitation shown in Figure 18. Among the possibilities which exist to reduce this velocity, radial guide vanes placed before the labyrinths (Figure 23) have in many cases helped to stabilize an originally unstable rotor. For the labyrinths on the balance piston another possibility exists in reducing the swirl velocity by supplying buffer gas from the discharge nozzle to the second labyrinth strip.

CONCLUSION

The vibrational behaviour of turbocompressor equipment is of great importance for the end-user. High efficiency and performance of a turbomachine become less important if it cannot be operated because of high vibrations. Therefore the design of turbocompressors must be based equally on aerothermodynamic and rotor dynamic considerations. It is obvious that in order to be able to optimize the rotor-dynamic qualities, reliable prediction of forced and self-excited vibrations is necessary. This calls for accurate modelling of the rotor-bearing system and realistic models of the excitation mechanisms. As it has been shown, the simulation of the rotor-bearing system today poses no serious problems, except possibly for the bearing support where further investigation may be necessary.

The problem of forced excitations caused by unbalance is solved by refined balancing techniques, which allows the reduction of the resulting vibrations to a minimum.

Aerodynamic mechanisms, such as rotating stall, may be eliminated in the operation range by selection of well-matched impellers and diffusers.

The dominant self-excitation mechanism has been shown to have its origins in the labyrinth seals. A reliable theoretical excitation model has been presented, which permits the calculation of the corresponding cross-coupling stiffnesses for different labyrinth geometries and operating conditions. A serious investigation of high-pressure compressors includes a stability analysis taking into account the labyrinth excitation. If poor stability margins are found, reduction of the excitation or an improved rotor-bearing design is necessary. In some cases, better stability properties can be obtained simply by selecting favorable bearing characteristics as bearing clearance and preload. To this end a parametric study has to be performed and this may be done by an approximate theory valid for most practical cases.

The best way to improve stability, however, is to reduce the cause for self-excitation. This may be done by suppressing the inlet swirl velocity of the leakage flow entering the labyrinth seals.

APPENDIX

APPROXIMATE ANALYSIS OF SELF-EXCITATION

Consider the rotor model in Figure A-1 with concentrated mass m, bearing distance l, shaft rigidity c_s, and bearing stiffness c and damping d, respectively. The excitation is given by the cross-coupling stiffness k and the resulting forces, acting in the middle plane of the rotor, read:

$$Q_x = -ky,$$
$$Q_y = kx,$$

where x and y are the horizontal and vertical rotor displacements, respectively. The rotor may be looked at as a plane single mass system (see Figure A-1) having the following equations of motion:

$$\begin{aligned} m\ddot{x} &= -c_s(x-x_B)-ky, \\ m\ddot{y} &= -c_s(y-y_B)+kx, \\ c_s(x-x_B) &= 2cx_B+2d\dot{x}_B, \\ c_s(y-y_B) &= 2cy_B+2d\dot{y}_B \end{aligned}$$

where x_B and y_B are the shaft displacements in the bearing

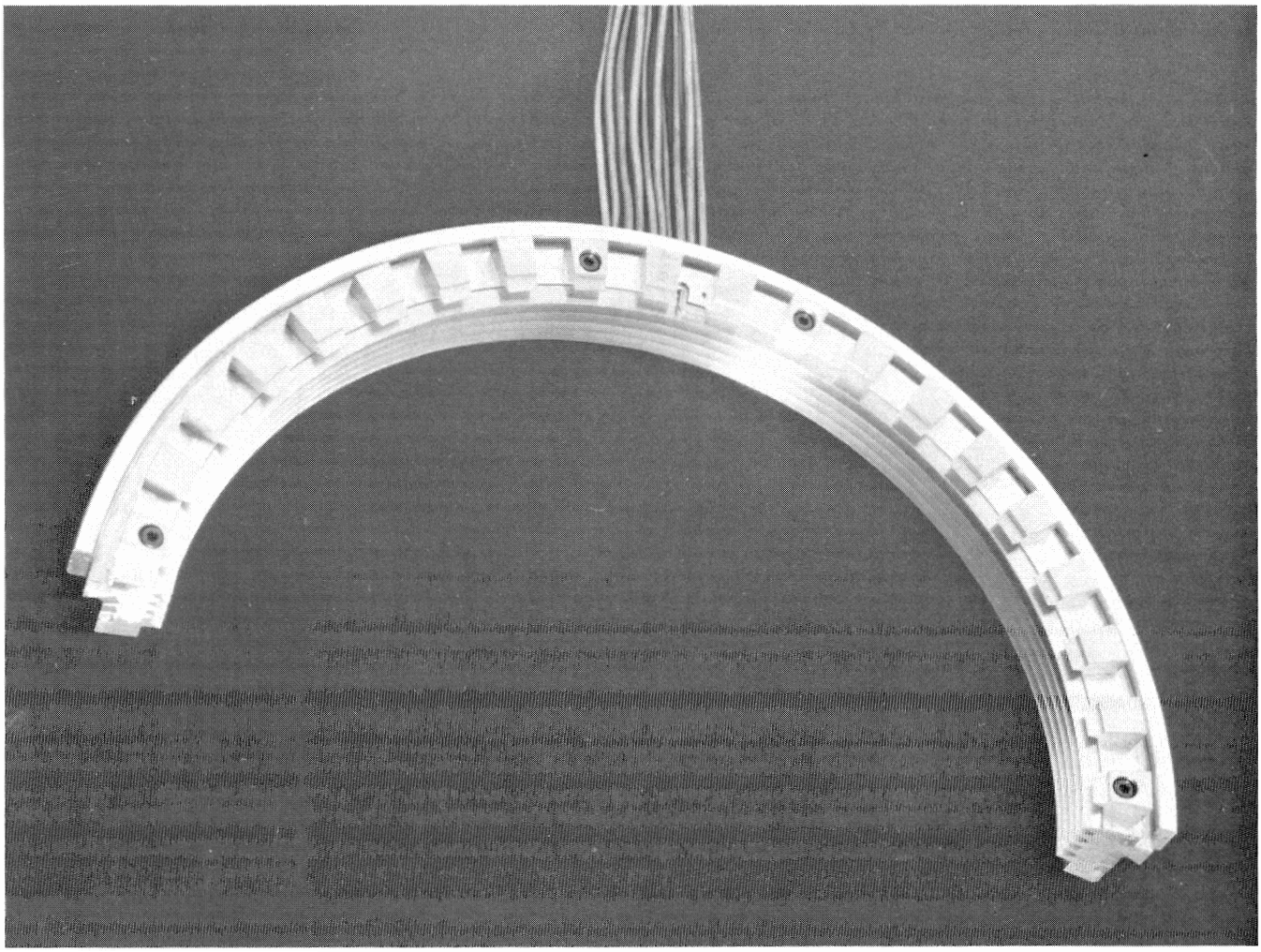

Figure 23. Radial Guiding Vanes.

planes. For a shaft with constant bending rigidity α, c_s is given by

$$c_x = \frac{48\alpha}{l^3} \quad .$$

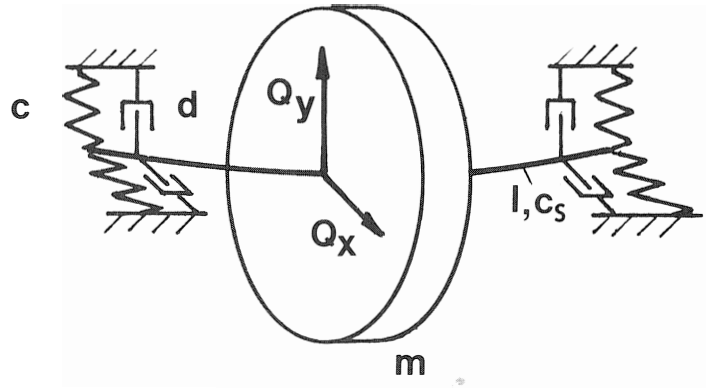

Eliminating x_B and y_B and setting

$$z = x + iy = \hat{z}e^{\lambda t}$$

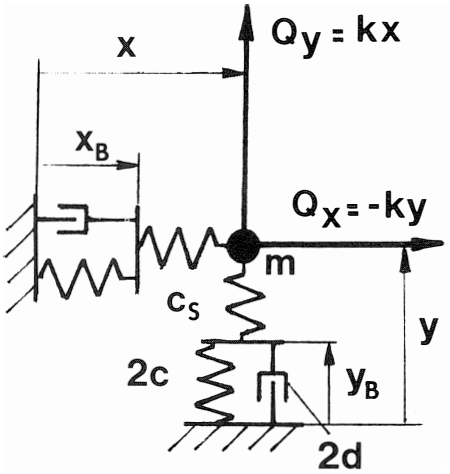

Figure (A-1). Rotor Model.

leads to

$$2d\lambda^3+(2c+c_s)\lambda^2+2\frac{d}{m}(c_s-ik)\lambda+\frac{2cc_s}{m}-\frac{ik}{m}(2c+c_s)=0\,. \quad \text{(A-1)}$$

For most rotor-bearing systems in technical applications the logarithmic damping decrement at zero excitation δ_0 is less than $0.1 \cdot 2\pi$. In this case the solutions of (A-1) may be obtained by expanding λ in powers of d:

$$\lambda=\lambda_0+d\lambda_1+d^2\lambda_2+\ldots.$$

Insertion in (A-1) and retaining only the terms of zeroth and first order in d gives: □

$$\lambda=\frac{\pm 1}{\sqrt{2m}}\left[\sqrt{\sqrt{\zeta^2+k^2}-\zeta}+i\sqrt{\sqrt{\zeta^2+k^2}+\zeta}\right]-\frac{d\zeta^2}{4mc^2}\,, \quad \text{(A-2)}$$

with

$$\zeta=\frac{2cc_s}{2c+c_s}$$

From (A-2) the natural frequency:

$$\omega=\sqrt{\frac{\sqrt{\zeta^2+k^2}+\zeta}{2m}} \quad \text{(A-3)}$$

and the logarithmic damping decrement δ are extracted:

$$\delta=\frac{2\pi}{\sqrt{\sqrt{\zeta^2+k^2}+\zeta}}\left[\frac{d\zeta^2}{2c^2\sqrt{2m}}\pm\sqrt{\sqrt{\zeta^2+k^2}-\zeta}\right]. \quad \text{(A-4)}$$

The rotor is stable as long as the bracket in (A-4) is positive. It is seen that only the forward motion may become unstable, because the negative sign of the second term in the bracket belongs to the positive natural frequency. Equations (A-3) and (A-4) may be simplified by linearisation of the k-dependence:

$$\omega=\sqrt{\frac{\zeta}{m}}\,, \quad \text{(A-5)}$$

$$\delta=\pi\left[\frac{d\zeta^2}{2c^2\sqrt{\zeta m}}-\frac{k}{\zeta}\right]\,. \quad \text{(A-6)}$$

Equation (A-6) may be expressed in terms of δ_0, the system damping at zero excitation, and ω, the undamped natural frequency:

$$\delta=\delta_0-k\frac{\pi^2 d\omega}{2c^2\delta_0}\,. \quad \text{(A-7)}$$

Equations (A-5) and (A-6) are good approximations for (A-3) and (A-4), respectively, as long as k/ζ is markedly smaller than 1. Hence, in this case the natural frequency is practically independent of the excitation k and the logarithmic decrement depends linearly on k.

REFERENCES

1. *Centrifugal Compressors for General Refinery Services*, API Standard 617, 4th ed. 1979.
2. Harris, C. M. and Crede C.E., *Shock and Vibration Handbook*, 2nd ed. (New York: McGraw-Hill, 1976).
3. Traupel, W., *Thermische Turbomaschinen*, 2nd ed. (Springer Verlag, 1968).
4. Gasch R. and Pfützner, H., *Rotordynamik* (Springer Verlag, 1975).
5. Thomas, H. J., "Instabile Eigenschwingungen von Turbinenläufern, angefacht durch die Spaltströmung in Stopfbuchsen und Beschaufelung", *Bull. Scientifique*, 71, No. 11/12 (1958), pp. 1039-1063.
6. Alford, J. S., "Protecting Turbomachinery From Self-Excited Whirl", *Journal of Engineering for Power*, Trans. ASME, Series A, 38 (1965), pp. 333-344.
7. Rosenberg, S. Sch., Orlik, W. G. and Marcenko, U. A., "Investigation of the Aerodynamic Transverse Forces in Labyrinth Seals with Eccentric Rotor", Energomasinostroenie, 8 (1974), pp. 15-17.
8. Benckert, H., "Spaltströmungen", *Forschungsberichte Forschungsvereinigung Verbrennungskraftmaschinen*, Vol. 253, 1978.
9. Kostyuk, A. G., "A Theoretical Analysis of the Aerodynamic Forces in the Labyrinth Glands of Turbomachines", *Teploenergetika (Thermal Engineering)*, 19 (1972), pp. 29-33.
10. Spurk, J. H. and Keiper, R., "Selbsterregte Schwingungen bei Turbomaschinen infolge der Labyrinthströmung", *Ing.-Arch.*, 43 (1974), pp. 127-135.
11. Urlichs, K., "Die Spaltströmung bei thermischen Turbomaschinen als Ursache für die Entstehung schwingungsanfachender Querkräfte", *Ing.-Arch.*,45 (1976), pp. 193-208.
12. Launder, B. E. and Spalding, D. B., *Mathematical Models of Turbulence*, (Academic Press, 1972).
13. Trutnovsky, K., *Berührungsfreie Dichtungen*(VDI-Verlag, 1973).